

Prostate intraepithelial neoplasia induced by prostate restricted Akt activation: The MPAKT model

Pradip K. Majumder^{*†‡}, Jen Jen Yeh^{*†‡}, Daniel J. George^{*†}, Phillip G. Febbo^{*†}, Jennifer Kum^{*†}, Qi Xue^{*†}, Rachel Bikoff^{*†}, Hongfeng Ma^{*†}, Philip W. Kantoff^{*†}, Todd R. Golub[§], Massimo Loda^{*¶}, and William R. Sellers^{*†||}

Departments of ^{*}Medical Oncology and [§]Pediatric Oncology, Dana–Farber Cancer Institute, and Departments of [†]Medicine and [¶]Pathology, Brigham and Women's Hospital, Harvard Medical School, Boston, MA 02115

Communicated by Lewis C. Cantley, Beth Israel Deaconess Medical Center, Boston, MA, April 15, 2003 (received for review January 7, 2003)

To determine whether Akt activation was sufficient for the transformation of normal prostate epithelial cells, murine prostate restricted Akt kinase activity was generated in transgenic mice (MPAKT mice). Akt expression led to p70^{S6K} activation, prostatic intraepithelial neoplasia (PIN), and bladder obstruction. mRNA expression profiles from MPAKT ventral prostate revealed similarities to human cancer and an angiogenic signature that included three angiogenin family members, one of which was found elevated in the plasma of men with prostate cancer. Thus, the MPAKT model may be useful in studying the role of Akt in prostate epithelial cell transformation and in the discovery of molecular markers relevant to human disease.

The insulin-like growth factor signaling pathway is implicated in both the initiation and progression of prostate cancer. For example, higher plasma insulin-like growth factor-1 levels are associated with prostate cancer risk, whereas inactivating somatic mutations of *PTEN* or loss of the PTEN protein are common in prostate cancer cell lines and in primary and metastatic tumor specimens (reviewed in ref. 1). The tumor suppressor activity of the lipid phosphatase PTEN is linked to its ability to antagonize phosphoinositide 3-kinase (PI3K) signaling (2). Thus, mutations in PTEN lead to deregulated PI3K signaling, resulting in constitutive activation of downstream targets including the Akt/PKB kinase family (Akt; reviewed in ref. 3). In keeping with these data, Akt kinase activity is frequently elevated in primary prostate tumors (4).

Akt is activated through membrane recruitment to sites of phosphatidylinositol 3,4,5-trisphosphate, through conformational change and through phosphorylation on residues Thr-308 and Ser-473 (3). Recruitment to the membrane as a gag-fusion (as in *v-akt*) or through the addition of a myristoylation sequence is sufficient both for kinase activation and for transformation of rodent and avian cells (5, 6).

When activated, Akt promotes both cell growth and cell survival. A growing number of substrates of Akt have been identified including glycogen synthase kinase-3 (GSK3), BCL2-antagonist of cell death protein (BAD), endothelial nitric oxide synthase (eNOS), Caspase 9, and I κ B kinase α (IKK α); however in *Caenorhabditis elegans* and *Drosophila melanogaster* genetic studies have specifically linked activation of Akt to the regulation of a Forkhead transcription factor and to activation of p70^{S6K}. In mammalian systems, restoration of Forkhead activity or inhibition of mTOR and p70^{S6K} reverses many aspects of the transformed phenotype resulting from the loss of PTEN (7–10).

PTEN^{+/-} mice develop prostate intraepithelial neoplasia (PIN) and microinvasive cancers (11, 12); however, viability is compromised as a result of extraprostatic disease. Recent data suggest that Akt1 may be necessary for the induction of a tumor phenotype in *PTEN*^{-/-} embryonic stem cells (13). Thus, to determine whether activation of Akt1 was sufficient for the induction of murine prostate cancer and to determine the extent to which such activation recapitulated the loss of PTEN in the murine prostate, transgenic mice were generated in which expression of activated Akt1 was spatially restricted to the

prostate. Expression of Akt1 in the ventral prostate (VP) of the MPAKT mice (murine prostate restricted Akt kinase transgenic mice) resulted in activation of the p70^{S6K} pathway and the induction of PIN similar in character to that observed in *PTEN*^{+/-} mice. These mice, although long-lived, develop bladder obstructions at a frequency of 30%, requiring euthanasia. Moreover, expression profiling revealed an angiogenic/hypoxia signature in these mice and the identification of an angiogenic plasma factor that was then validated in plasma samples taken from patients with prostate cancer.

Materials and Methods

Generation of Akt Expressing Transgenic Lines. The insert from pCDNA3-myr-HA-Akt1 was liberated by *EcoRI/XbaI* digestion, blunted, and ligated to *EcoRV* restricted pBSK-rPb carrying -426 to +28 of the rat probasin promoter (19). The linearized rPb-myr-HA-Akt1 insert was injected into pronuclei of fertilized oocytes, and 10 FVB founders were identified.

Genotyping, Dissections, and Preparation of Tissues. Isolation of tail DNA, PCR-based genotyping, prostate and genitourinary tract dissections, tissue fixation, and hematoxylin/eosin (H&E) staining were performed as described in the methods available at <http://research.dfci.harvard.edu/sellerslab/datasets/index.html>. *PTEN* mice were genotyped as described (11).

Immunohistochemical Analysis. Mounted tissue sections were hydrated, incubated for 30 min with 3% H₂O₂ in methanol at room temperature, washed with double distilled water and PBS, and heated in a microwave to 199°F in 1 mM EDTA (pH 8.0) for 25 min (for anti-PTEN, anti-ppS6, and anti-ppAKT staining), or in 10 mM citrate buffer (pH 6.0) for 30 min (for anti-p63 staining), or heated in a pressure cooker in 10 mM citrate buffer (pH 6.0) for 30 min (for anti-ppGSK3 staining), or incubated with 0.25% trypsin for 30 min at 37°C (for anti-CD31 staining). Sections were blocked in 10% goat serum (Vector Laboratories; 30 min), incubated with anti-Akt-pS473 (1:400), anti-ppGSK3 β (pS9; 1:25), anti-ppS6 (pS235/236; 1:400), antisera (Cell Signaling Technology, Beverly, MA), anti-PTEN antisera (1:600; ref. 14), anti-p63 antisera (1:100; BD PharMingen), or anti-CD31-PECAM antisera (1:100; BD PharMingen) in 1% BSA (12 h at 4°C), washed with PBS, and incubated with secondary antibody (1:200; Vector Laboratories; 30 min). Antigen–antibody complexes were detected with the ABC kit (Vector Laboratories).

Immunoblot Analysis. Proteins from fresh tissues were extracted in TNN buffer (50 mM Tris, pH 7.4/150 mM NaCl/0.5% Nonidet

Abbreviations: PIN, prostate intraepithelial neoplasia; MPAKT, murine prostate restricted Akt kinase transgenic; VP, ventral prostate; PSCA, prostate stem cell antigen; ISH, *in situ* hybridization; HA, hemagglutinin; myr, myristoylated; LP, lateral prostate; IHC, immunohistochemical analysis; GSK, glycogen synthase kinase.

^{*}P.K.M. and J.J.Y. contributed equally to this work.

^{||}To whom correspondence should be addressed at: Dana–Farber Cancer Institute, D720C, 44 Binney Street, Boston, MA 02115. E-mail: William.Sellers@dfci.harvard.edu.

P-40/5 mM EDTA, pH 8.0/1 mM NaOAc/1 mM DTT/5 mM NaF/5 μ g/ml leupeptin/5 μ g/ml aprotinin/1 mM PMSF), separated by gel electrophoresis, transferred, and immunoblotted as described (7). Anti-Akt-S473, anti-pan-Akt, anti-GSK3-S9, anti-pan GSK3 (Cell Signaling Technology) were used at 1:1,000, and anti-hemagglutinin (HA) (Santa Cruz Biotechnology) was used at 1:2,000.

RNA Isolation and Microarray Expression Analysis. Total RNA was prepared from VP by the Trizol method (Invitrogen). The generation of biotinylated target cRNA (using 15 μ g of total RNA per sample) fragmentation, hybridization to the Affymetrix Murine U74Av2 arrays, washing, and scanning were carried out as described (15). Raw expression values were normalized to the array intensity of array 1. Genes whose expression varied <5-fold between any two samples in the experiment were filtered. Genes differentially expressed between the four transgenic and four wild-type VPs were ranked by using a modified signal-to-noise metric calculated as follows: $|\chi_{akt} - \chi_{wt}|/(\sigma_{akt} + \sigma_{wt})$ (16).

In Situ Hybridization. A 316-bp PCR product for angiogenin-3 was generated by RT-PCR using the oligonucleotides and 5'-TTAACCTCACTAAAGGGACCAGGACGACGACGAGCTAGAC-3' and 5'-TAATACGACTCACTATAGGGCACA-GATGGCCTTGATGTTG-3', which include T7 and T3 polymerase binding sites. A cRNA probe for prostate stem cell antigen (PSCA) was generated as described (17). Digoxigenin-labeled (PSCA) and radiolabeled (angiogenin-3) riboprobes were generated, and *in situ* hybridization (ISH) was carried out as described (18).

Analysis of Plasma Levels of Angiogenin in Clinical Samples. Plasma samples were collected from consenting individuals with clinically localized prostate cancer (39 patients), metastatic, hormone-refractory (40 patients), or no history of prostate cancer (37 patients). Plasma angiogenin levels were determined after an 800-fold dilution in duplicate by using a Quantiglo chemiluminescent ELISA kit (R & D Systems). Descriptive statistics were used to characterize each category of subjects. Wilcoxon rank-sum tests were used to assess the pair-wise differences between categories. Because each group was used in two comparisons, a *P* value of 0.025 was considered statistically significant. To assure that the conclusions were robust to method of analysis, a second method of analysis was applied. Specifically, the data were log transformed, resulting in a more normal distribution. The 95% confidence intervals were then generated for the natural log-transformed angiogenin levels for each group.

Results and Discussion

Expression of Activated Akt Spatially Restricted to the VP. After pronuclear injections of a plasmid insert containing -421 to +28 of the probasin promoter (19) upstream of a cDNA for HA epitope-tagged, myristoylated (myr), human Akt-1 (Fig. 1A), 10 founders harboring at least one copy of the transgene were identified by Southern blotting (data not shown). All founders were backcrossed to the FVB parental strain (Fig. 1B), and representative transgene-bearing F₁ males were killed at 8 wk. RNA and protein of ventral, lateral, dorsal, and anterior prostate lobes were isolated, and evidence for transgene expression and protein production was sought by RT-PCR and anti-HA immunoblotting. A single line, MPAKT was found to have prostate-specific expression of HA-myr-Akt1 mRNA and protein (Fig. 1C and data not shown). The prostate lobes of all of the F₁ offspring from the nonexpressing lines were normal when evaluated histologically and were not evaluated further (data not shown).

Next, protein extracts from tissues of the genitourinary tract were harvested from 8-wk-old MPAKT and littermate control

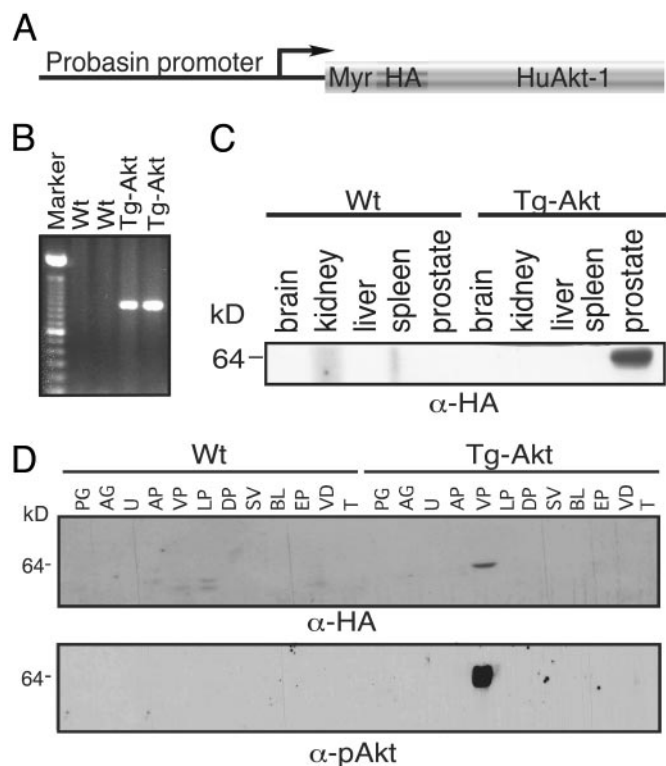


Fig. 1. Akt activation is spatially restricted to the prostate. (A) Schematic diagram of the Akt-1 transgene. A cDNA directing the expression of myr and HA epitope-tagged human Akt-1 was inserted 3' of the rat probasin promoter, -426 to +28 bp. (B) PCR-based genotyping of representative transgenic founders (Tg) or controls (Wt). (C) Prostate-specific transgene expression. Protein extracts from the indicated tissues from wild-type (Wt) and transgenic (Tg-Akt) mice were immunoblotted by using anti-HA antibody. (D) Transgene-directed Akt expression predominantly in the VP. Protein extracts prepared from the indicated genitourinary tract tissues (PG, preputial gland; AG, ampullary gland; U, urethra; VP, ventral prostate; LP, lateral prostate; DP, dorsal prostate; SV, seminal vesicle; BL, bladder; EP, epididymis; VD, vas deferens; and T, testis) from 8-wk-old wild-type (Wt) and transgenic (Tg-Akt) mice were immunoblotted with anti-HA antibody (Upper) or reprobbed with anti-pS473 (Lower).

males and probed with anti-HA antibody. HA-myr-Akt1 protein was uniformly detected in the VP, and, in 10% of MPAKT mice, low-level expression was detected in the lateral prostate (LP; see also Fig. 2E and F). Expression was not detected in any other tissue (Fig. 1D Upper).

To determine the activation state of the Myr-HA-Akt1, immunoblots were probed with antisera against phospho-S473 of Akt and with pan-Akt antisera. Endogenous Akt and Myr-HA-Akt1 were found in equivalent amounts; however, only Myr-HA-Akt1 was phosphorylated (Figs. 1D Lower and 2A). Similarly, genitourinary tract tissues of MPAKT and control males were fixed, embedded, and subject to immunohistochemical analysis (IHC) by using anti-pS473 antisera. Marked plasma membrane and cytoplasmic staining was seen in the VP of MPAKT, but not in littermate controls (Fig. 2C and D). In addition, focal pS473 staining of the LP was observed in a minority of transgenic males (Fig. 2E and F). To determine the phosphorylation state of a downstream substrate of Akt, proteins and tissues isolated from both MPAKT and littermate control mice were immunoblotted or studied by IHC with antisera to phospho-S9 of GSK3 or total GSK3. Phosphorylation of GSK3 was detected by both methods in the VP of MPAKT males (Fig. 2B, G, and H) and in tissue sections staining of phospho-S9 colocalized with anti-S473 staining. Finally, protein extracts

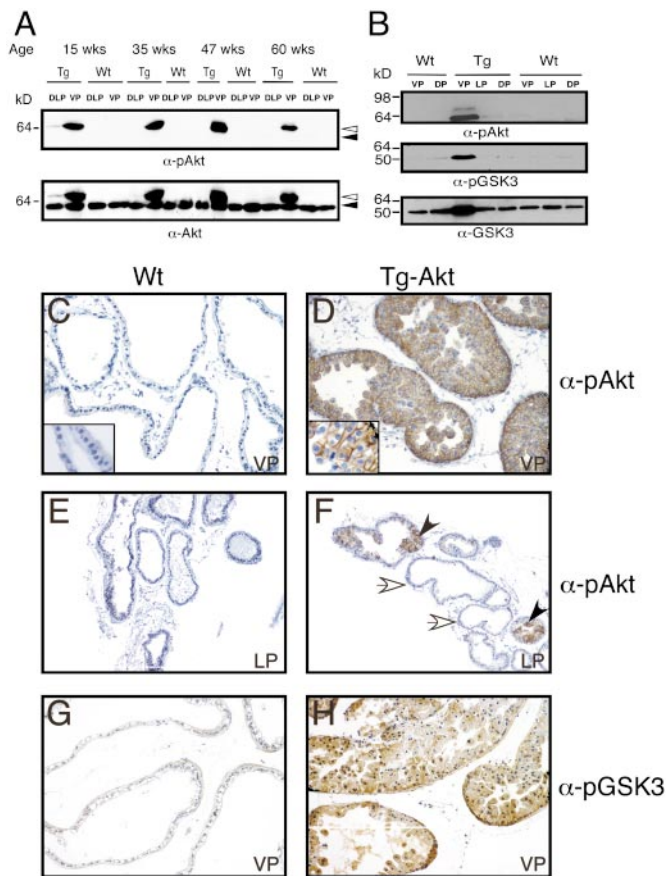


Fig. 2. Activation of Akt and phosphorylation of GSK3. (A) Protein lysates from dorsolateral (DLP) and VP of MPAKT (Tg) and wild-type (Wt) littermate mice at 15, 35, 47, and 60 wk were immunoblotted with anti-p5473 (Upper) and pan-Akt (Lower) antisera. The positions of endogenous murine Akt (filled arrow) and myr-HA-Akt-1 (open arrow) are indicated. (B) Protein lysates from VP, DP, and LP from MPAKT and wild-type mice were immunoblotted with anti-p5473 (Top), anti-phospho-GSK3 (pS9; Middle), and anti-pan GSK3 (Bottom). (C–H) IHC staining of tissue sections from VP or LP from wild-type (Wt) and MPAKT (Tg-Akt) with anti-p5473 or anti-phospho GSK-3 (pS9) antisera as indicated (C–H, $\times 200$; Insets C and D, $\times 400$).

prepared from the VP of mice killed at 15, 35, 47, and 60 wk were probed with anti-pan-Akt and anti-pS473 antisera. Here, expression and activation of Akt could be demonstrated in mice spanning all ages (Fig. 2A). Of note, expression and activation of Myr-HA-Akt1 in MPAKT mice can be detected as early as 2 days postnatal (Fig. 6, which is published as supporting information on the PNAS web site, www.pnas.org). Together, these data suggest that constitutive activation of Akt1 and phosphorylation of a known Akt substrate have been achieved in a predominantly VP-restricted pattern.

Akt Expression and Activation Is Sufficient for the Induction of PIN. Histologic study of the VP of the MPAKT line revealed a striking phenotype characterized by a hyperplastic and dysplastic epithelium with disorganized multicell layers, intraepithelial lumen formation, loss of cell polarity, nuclear atypia, and apoptotic bodies (Fig. 3A–D; and Figs. 7 and 8, which are published as supporting information on the PNAS web site) (20, 21). These histopathologic features are consistent with PIN and were confirmed in independent review by three expert pathologists.

No abnormalities were seen in the dorsal or anterior prostate of the MPAKT mice. However, in the instances where phosphorylated Akt was focally expressed in the LP, coincident focal

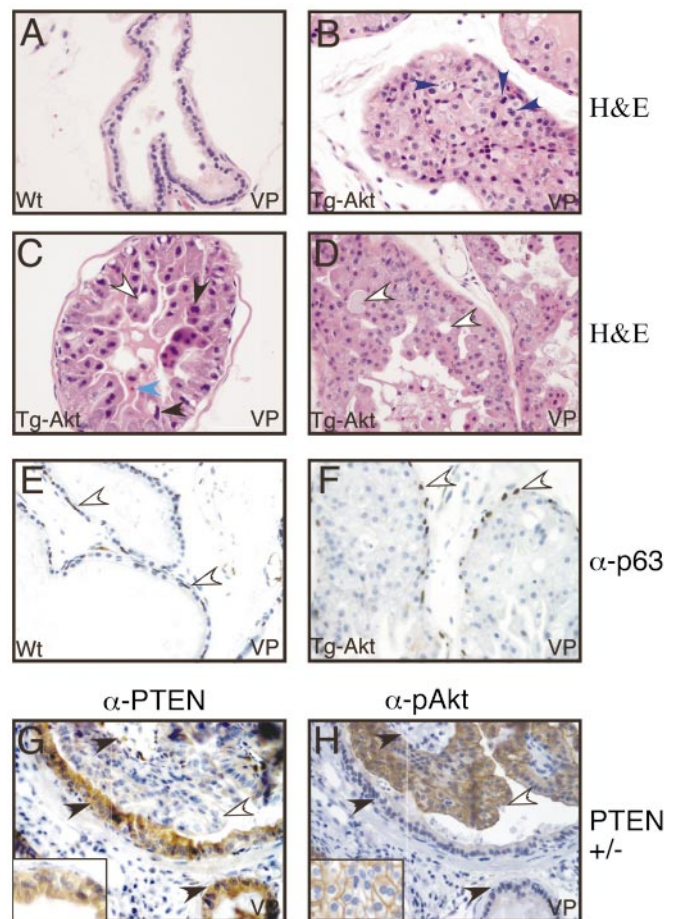


Fig. 3. Akt activation induces PIN. (A–D) Akt induced PIN in the VP. VP from both Wt (A) and MPAKT (Tg-Akt; B–D) mice were stained with hematoxylin/eosin. Features of dysplasia indicative of PIN include loss of cell polarity (B–D), mitotic figures (blue arrows in B), nuclear atypia (black arrows in C), apoptotic bodies (light blue arrow in C), and intraepithelial lumen formation (white arrows in C and D). (E and F) Preservation of the basal cell layer in MPAKT VP. Tissue sections of VPs from Wt (E) and MPAKT (F) mice were stained with anti-p63. Arrows indicate representative p63-positive basal cells. (G and H) Concordance of Akt activation and PIN in the VP of PTEN heterozygous mice. Sequential tissue sections from the VP of PTEN heterozygous mice were stained with anti-PTEN (G) and anti-p5473 (H). Areas of positive anti-PTEN staining accompanied by negative anti-p5473 staining (filled arrows) whereas areas with loss of PTEN staining accompanied by positive anti-p5473 staining (open arrows) are indicated (compare G with H). (A–F, $\times 400$; G and H, $\times 200$; Insets, $\times 400$).

PIN was noted in these areas (Fig. 2E and F). In addition, rarely areas of the VP in MPAKT mice failed to express Akt, and in this setting there was no evidence of PIN (data not shown). Thus, there is a direct correlation between transgene expression, activation of Akt, and the development of PIN. These latter data strongly suggest that this phenotype is a direct result of the expression and function of Akt kinase activity and is unlikely to have been caused by a gene activation or inactivation event resulting from the integration of the transgene.

Human PIN lesions are characterized by preservation of the basement membrane and the basal cell layer. In the murine prostate, basal cells are similarly aligned circumferentially around the secretory epithelium. The p53 family member p63 is a highly specific basal cell marker that, in the mouse, is necessary for the appropriate maintenance of prostate basal cells (22). In keeping with observations made in human PIN, IHC staining for p63 revealed normal numbers and organization of the basal cell

layer in the VPs from both control FVB and MPAKT mice (Fig. 3 *E* and *F*).

Akt Activation Leads to Activation of the p70^{S6K} Pathway, Increases in Prostate Epithelial Cell Size, and Urinary Bladder Obstruction. The PIN lesions observed in the MPAKT line seem to result from both an increase in cell number (a mean of 26.7×10^4 WT vs. 98.3×10^4 MPAKT) and an increase in cell size (a mean of $10.7 \pm 1.6 \mu\text{m}$ WT vs. $15.74 \pm 3.3 \mu\text{m}$ MPAKT) (Fig. 4*G*). This phenotype seen in *D. melanogaster* harboring PTEN mutations (23, 24) and in PTEN^{+/-} mice has been linked to the activation of p70^{S6K} (8). In keeping with these data, robust cytoplasmic staining for the p70^{S6K} substrate phospho-RPS6 (ppS6) was seen in the VP of MPAKT but not in WT males and colocalized with anti-Akt pS473 staining (Fig. 4 *A* and *B*). Likewise, in the LP ppS6, staining colocalized with areas of focal PIN and with focal staining of phospho-Akt (Fig. 4 *C* and *D*). These data suggest that the activation of Akt results in the activation of p70^{S6K} and is linked to the development of PIN in MPAKT mice.

The MPAKT PIN phenotype was markedly distinct from the pathological changes seen in transgenic adenocarcinoma of the mouse prostate (TRAMP) mice where a cribriform intraepithelial hyperplasia containing smaller cells with hyperchromatic nuclei is detected at 10 wk and invasive adenocarcinoma is detected at 20 wk (19), but was similar, although more uniform and extensive, to that seen in PTEN^{+/-} mice. In these mice (11), we found that the prostate histology remained normal until 38 wk whereupon focal loss of PTEN protein was detected by IHC (in VP, LP, and dorsal prostate; Fig. 3*G*) along with coincident gain of anti-pS473 staining (Fig. 3*H*). In these areas, focal PIN lesions were found that were similar in histological appearance to those seen with Akt expression. In these lesions, activated endogenous Akt was localized primarily to the plasma membrane with a marked absence of nuclear staining, and, as seen in the MPAKT mice, phosphorylation of S6 was coincident with the activation of Akt (Fig. 4 *E* and *F*). These data suggest a marked overlap in the phenotype induced by activation of Akt and that resulting from loss of PTEN, and are consistent with the results of transgenic Akt1 expression in other organs (25–28).

Kaplan-Meier analysis showed minimal overall differences in survival between transgenic and nontransgenic littermates (Fig. 4*H*). However, older mice (15/41 transgenic mice vs. 0/23 WT mice) developed a protuberant abdomen as a result of a bladder outlet obstruction and were killed, resulting in a decrease in survival at later time points (Fig. 4 *I* and *J*). Sectioning of the urethra revealed an obstruction at the level of the prostate (data not shown). To date, histological examination of mice at 8, 17, 27, 45, 60, and 78 wk has failed to identify evidence of invasive cancer, including 41 transgenic mice aged 78 wk or older (Fig. 6). PTEN heterozygous mice do develop prostate adenocarcinomas (29), and, whereas Akt expression is sufficient to induce PIN, it is not sufficient for the induction of overt tumors in this strain of mice, suggesting that additional oncogenic events are required *in vivo* for progression to adenocarcinoma. The difference in the prostate phenotype between MPAKT and PTEN^{+/-} mice (PIN vs. invasive cancer) may arise as a result of growth/survival advantages conferred through loss of PTEN and not simply reproduced by activation of Akt. Alternatively, strain-specific differences between the C57BL/6 background of the PTEN^{+/-} mice and the FVB background of the MPAKT mice might account, at least in part, for a difference in the phenotype. Expression profiling data from our lab have revealed surprisingly strong strain-specific expression differences in the ventral prostate, strong enough that FVB and C57BL/6 segregate in self-organized maps (P.K.M. and W.R.S., unpublished results). Moreover, initial crosses of MPAKT on to the C57BL/6 background have revealed an increase in BrdUrd incorporation compared with the FVB strain (data not shown). Because

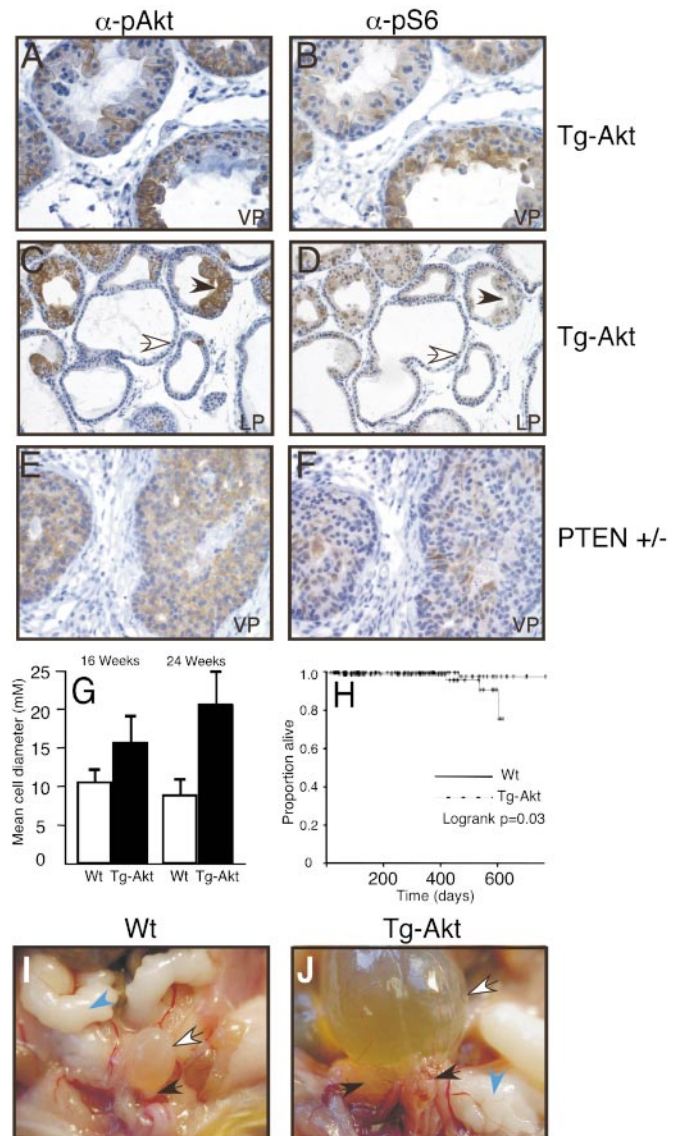


Fig. 4. Prostate expression of Akt induces activation of the p70^{S6K} pathway, leads to increased cell and organ size, and induces bladder outlet obstruction. (*A–D*) Activation of S6 is coincident with activation of Akt. Sequential tissue sections from VP or LP from MPAKT mice were stained with anti-pS473 and anti-pS6 (as indicated). Filled and open arrows indicate representative costained and co-unstained regions of LP, respectively. (*E* and *F*) Coincident phosphorylation of Akt and S6 in the prostate of PTEN^{+/-} mice. Sequential sections of VP were stained with the indicated antisera. (*G*) Transgenic expression of Akt results in an increase in cell size. Hematoxylin/eosin-stained tissue sections from VP of MPAKT (Tg-Akt) and wild-type (Wt) littermate control mice at 16 wk and 24 wk of age were used to obtain the bidimensional measurements of all secretory epithelial cells. The mean and SD of the cell diameter (μm) from 10 animals of each genotype are shown. (*H*) MPAKT mice have a normal life span. Kaplan–Meier survival analysis of wild-type (Wt, solid line) and MPAKT (Tg-Akt, dashed line) mice. (*I* and *J*) Representative genitourinary tract of a nonobstructed Wt control compared with a MPAKT male with bladder obstruction. The white arrows indicate the bladder, blue arrows indicate seminal vesicles, and the black arrows indicate VP. (*A*, *B*, *E*, and *F*, $\times 400$; *C* and *D*, $\times 200$; *I* and *J*, $\times 4$.)

MPAKT mice do not suffer the consequence of an extraprostatic phenotype, this model provides an opportunity to study mutagenic, environmental, dietary, and possible strain-related or other genetic factors that may cooperate with activation of Akt to induce prostate tumorigenesis.

Expression Profiling and Angiogenesis in Transgenic Prostate. To determine whether the epithelial cells expanded within the PIN lesions observed in the MPAKT animals were similar at a molecular level to prostate epithelial cells found in human prostate cancer, the patterns of gene expression in MPAKT vs. nontransgenic animals were analyzed. To this end, total RNA was isolated from the VP of four MPAKT and four littermate control mice at 8 wk. Labeled cRNA was generated and hybridized to the Affymetrix U74Av2 murine expression array. Average difference values generated by using the MAS4 software (Affymetrix, Santa Clara, CA) were scaled (scaling factors ranged from 0.79–1.8). Genes were filtered to eliminate those that had less than 5-fold variation between the maximum and minimum values across the eight samples. The expression differences between FVB and MPAKT mice were sufficiently robust to allow for the unsupervised separation of FVB and MPAKT mice by hierarchical clustering (data not shown). Genes whose expression pattern was strongly correlated with the class distinction MPAKT vs. WT (FVB) were ranked by using a modified signal-to-noise metric and statistical significance assessed by permutation testing. Up-regulated genes (350) and 175 down-regulated genes exceeded the 5% permutation threshold. The top 50 up- and down-regulated genes are shown in Fig. 5A, and the list of the top 100 up- and down-regulated genes is shown in Tables 1 and 2, which are published as supporting information on the PNAS web site. All raw and normalized data can be found in Tables 3 and 4, which are published along with cel files as supporting information on the PNAS web site. All raw and normalized data and cel files also are available at <http://research.dfci.harvard.edu/sellerslab/datasets/index.html>.

Among the most significantly up-regulated genes was PSCA, a gene that is expressed in prostate ductal tips during prostate development (17). In human prostate cancers, PSCA levels both at the mRNA and protein level are increased (30). Moreover, PSCA induction has been reported in PTEN^{+/-} mice as well (31). The gene for osteocalcin (or gla protein), a gene also up-regulated in primary prostate cancer (32) and present in the serum of men with metastatic prostate cancer (33), was also strongly up-regulated (27-fold) in the expression profiles from the MPAKT mice (Fig. 5A and Table 1). ISH using a PSCA cRNA probe revealed robust staining of MPAKT, but not nontransgenic VP, confirming the differential expression of PSCA observed in the expression profiling (Fig. 5B and C). These data suggest that multiple markers of human prostate cancer are expressed in this model.

Angiogenin-3 had the highest signal-to-noise score and was induced 32-fold (Table 1). Angiogenin-3 is a member of a family of secreted proteins that induce angiogenesis, and that includes angiogenin-related protein and angiogenin-1, both of which were also overexpressed (10- and 3-fold induction, respectively; Table 1). Additional proangiogenic factors or hypoxia-induced genes that were strongly induced included FGF-BP1 (12.5 fold), endothelin-1 (5-fold), NIP3 (4.6-fold), and hypoxia-induced gene 1 (Hig1; 3.3-fold). Angiogenin-3 overexpression was confirmed by ISH; however, in contrast to the results for PSCA, expression was localized primarily to epithelial cells juxtaposed to the basement membrane (Fig. 5D and E). Together, these data strongly suggested that Akt-induced PIN might be associated with neovascularization. In keeping with this idea, CD31 staining revealed an extensive vasculature in the VP of MPAKT mice compared with nontransgenic controls (Fig. 5F and G).

The Angiogenins in Human Prostate Cancer Patients. The angiogenic signature found in these early PIN lesions raised the possibility that a number of these secreted factors might be elevated in patients with prostate cancer. In the human genome, there is only one angiogenin (Ang1). Angiogenin-3 (Mm.24663) is 80% homologous to human angiogenin-1, and there is no other

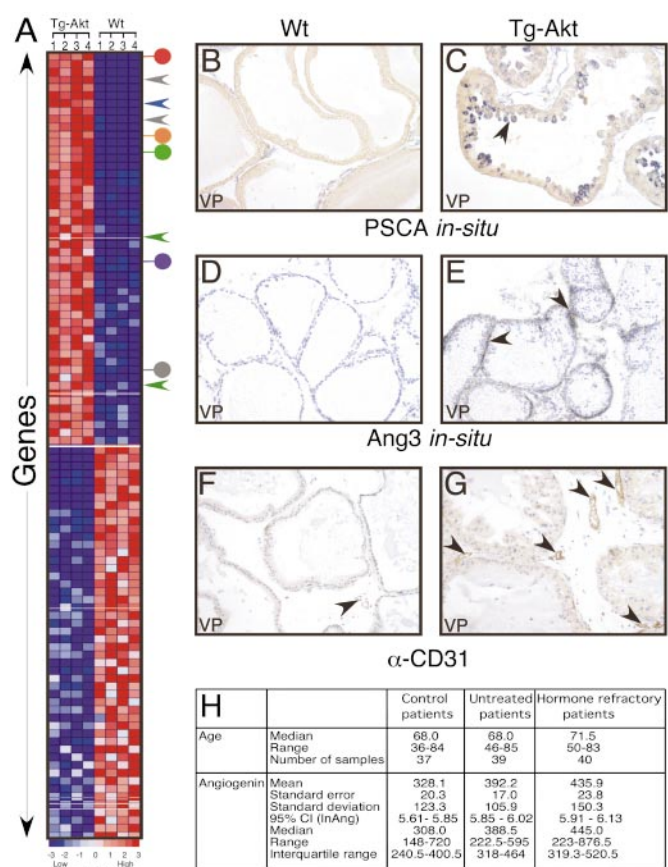


Fig. 5. Identification of novel tissue and serum markers in transgenic VP. (A) Differential gene expression detected on oligonucleotide microarrays. Genes differentially up- (Upper) or down- (Lower) regulated between the four transgenic and four wild-type littermate control were ranked by a signal-to-noise metric. Columns indicate individual RNA samples whereas rows represent specific mRNAs (as indicated). Relative expression levels are depicted as SD above (red) or below (blue) the mean value for the experiment. Hypoxia-regulated genes or those known to play a role in angiogenesis are indicated by the following circles: angiogenin-3 (red), fibroblast growth factor binding protein 1 (FGF-BP1) (orange), angiogenin-related protein (green), Bcl2/adenovirus E1B 19-kDa protein-interacting protein 3 (NIP3) (blue), and endothelin-1 (gray). The rows representing the genes for osteocalcin (gray) and PSCA (blue) are indicated by arrows. (B–G) Validation of expression differences. PSCA (B and C) and angiogenin3 (Ang3; D and E) were visualized by ISH. Black arrows indicate representative positively stained cells. (F and G) Angiogenesis in the VP of MPAKT. Tissue sections of the VP from MPAKT (Tg-Akt) and wild-type (Wt) littermate animals were stained with anti-CD31 antibody. The black arrows indicate representative stained vessels. (H) Plasma angiogenin level in clinical samples. Plasma level of angiogenin (pg/ml) in controls, untreated prostate cancer patients, and hormone refractory prostate cancer patients as indicated (B–G, $\times 200$).

apparent homolog. Therefore, angiogenin-1 levels were determined in plasma collected from patients with hormone-refractory prostate cancer (40 patients), newly diagnosed, untreated prostate cancer (39 patients), and from control patients with no evidence of prostate cancer (37 patients). Whereas there was significant variation in angiogenin levels, there was a statistically significant difference in angiogenin levels between the cancer groups and the non-cancer groups. Specifically, there was a statistically significant difference between controls and untreated, hormone-naive prostate cancer patients ($P = 0.01$) and between controls and hormone refractory prostate cancer patients ($P = 0.0009$). There was a trend toward higher levels of angiogenin in hormone refractory patients compared with un-

treated patients that did not reach statistical significance ($P = 0.27$). Therefore, angiogenin levels are higher in prostate cancer patients than in men without prostate cancer (Fig. 5H).

The question remains as to whether this signature reflects a direct activity of Akt. There have been a number of connections made between phosphoinositide 3-kinase signaling, PTEN loss, Akt activation, and the regulation of hypoxia-induced factor 1 (HIF-1) (34, 35). On the other hand, the marked segregation of angiogenin-3 expression to cells juxtaposing the basement membrane raises the possibility that this angiogenic signature may reflect a generalized transcriptional response to the proliferative PIN lesions. If so, this result may reflect a HIF-1-independent response as the mRNAs for HIF itself and for typical HIF transcriptional targets such as Glut-1 were not induced. An important future step will be to elucidate the details of this mechanism.

Endothelin-1 is elevated in PIN lesions and in the plasma of men with prostate cancer (36, 37). The finding that angiogenin is likewise elevated in the plasma of prostate cancer patients suggests that the MPAKT model recapitulates a number of elements commonly seen in human disease. Indeed, three independent secreted proteins (osteocalcin, endothelin-1, and angiogenin) are all overexpressed in this model and are found in the

serum of patients with prostate cancer. These observations support the idea that the MPAKT model recapitulates certain elements of the prostate cancer disease phenotype, and, consequently, this mouse model may prove useful in the discovery of novel prostate cancer markers.

The robust nature and uniform penetration of the PIN phenotype and of the transcriptional profile, together with the lack of an extraprostatic phenotype and the maintenance of the phenotype in the heterozygous state, combine to make this a useful model in which to test both novel small molecular inhibitors of Akt, of TOR signaling, and of proteins (such as angiogenin) involved in the generation of an angiogenic response.

We thank James Horner and Ronald DePinho for expert assistance in generating the transgenic founders; Judy Shim, Nandita Bhattacharya, Yang Yu, and Christine Ladd for their excellent technical assistance; Mark A. Rubin and Sabina Signoretti for reviewing the histology of the MPAKT mice; Dr. Pier Paolo Pandolfi and Antonio Di Cristofano for providing the PTEN^{+/-} mice; and Norman Greenberg for the rat probasin promoter. This work was supported by National Cancer Institute Grant PO1 CA89021, by the Association for the Cure of Cancer of the Prostate (CaPCURE), and by a Damon Runyon Clinical Investigator Award (to W.R.S.).

1. Sellers, W. R. & Sawyers, C. A. (2002) in *Prostate Cancer Principles and Practice*, ed. Kantoff, P. (Lippincott Williams & Wilkins, Philadelphia).
2. Nakamura, T. & Dixon, J. E. (1998) *J. Biol. Chem.* **273**, 13375–13378.
3. Vazquez, F. & Sellers, W. R. (2000) *Biochim. Biophys. Acta* **1470**, M21–M35.
4. Sun, M., Wang, G., Paciga, J. E., Feldman, R. I., Yuan, Z. Q., Ma, X. L., Shelley, S. A., Jove, R., Tschlis, P. N., Nicosia, S. V. & Cheng, J. Q. (2001) *Am. J. Pathol.* **159**, 431–437.
5. Bellacosa, A., Testa, J. R., Staal, S. P. & Tschlis, P. N. (1991) *Science* **254**, 274–277.
6. Staal, S. P. (1987) *Proc. Natl. Acad. Sci. USA* **84**, 5034–5037.
7. Nakamura, N., Ramaswamy, S., Vazquez, F., Signoretti, S., Loda, M. & Sellers, W. R. (2000) *Mol. Cell. Biol.* **20**, 8969–8982.
8. Podyspanina, K., Lee, R. T., Politis, C., Hennessy, I., Crane, A., Puc, J., Neshat, M., Wang, H., Yang, L., Gibbons, J., et al. (2001) *Proc. Natl. Acad. Sci. USA* **98**, 10320–10325.
9. Neshat, M. S., Mellinghoff, I. K., Tran, C., Stiles, B., Thomas, G., Petersen, R., Frost, P., Gibbons, J. J., Wu, H. & Sawyers, C. L. (2001) *Proc. Natl. Acad. Sci. USA* **98**, 10314–10319.
10. Aoki, M., Blazek, E. & Vogt, P. K. (2001) *Proc. Natl. Acad. Sci. USA* **98**, 136–141.
11. Di Cristofano, A., Pesce, B., Cordon-Cardo, C. & Pandolfi, P. P. (1998) *Nat. Genet.* **19**, 348–355.
12. Podyspanina, K., Ellenson, L. H., Nemes, A., Gu, J., Tamura, M., Yamada, K. M., Cordon-Cardo, C., Catorretti, G., Fisher, P. E. & Parsons, R. (1999) *Proc. Natl. Acad. Sci. USA* **96**, 1563–1568.
13. Stiles, B., Gilman, V., Khanzenon, N., Lesche, R., Li, A., Qiao, R., Liu, X. & Wu, H. (2002) *Mol. Cell. Biol.* **22**, 3842–3851.
14. Ramaswamy, S., Nakamura, N., Vazquez, F., Batt, D. B., Perera, S., Roberts, T. M. & Sellers, W. R. (1999) *Proc. Natl. Acad. Sci. USA* **96**, 2110–2115.
15. Singh, D., Febbo, P. G., Ross, K., Jackson, D. G., Manola, J., Ladd, C., Tamayo, P., Renshaw, A. A., D'Amico, A. V., Richie, J. P., et al. (2002) *Cancer Cell* **1**, 203–209.
16. Bhattacharjee, A., Richards, W. G., Staunton, J., Li, C., Monti, S., Vasa, P., Ladd, C., Beheshti, J., Bueno, R., Gillette, M., et al. (2001) *Proc. Natl. Acad. Sci. USA* **98**, 13790–13795.
17. Reiter, R. E., Gu, Z., Watabe, T., Thomas, G., Szigeti, K., Davis, E., Wahl, M., Nisitani, S., Yamashiro, J., Le Beau, M. M., et al. (1998) *Proc. Natl. Acad. Sci. USA* **95**, 1735–1740.
18. Signoretti, S., Montironi, R., Manola, J., Altimari, A., Tam, C., Bubley, G., Balk, S., Thomas, G., Kaplan, I., Hlatky, L., et al. (2000) *J. Natl. Cancer Inst.* **92**, 1918–1925.
19. Greenberg, N. M., DeMayo, F., Finegold, M. J., Medina, D., Tilley, W. D., Aspinall, J. O., Cunha, G. R., Donjacour, A. A., Matusik, R. J. & Rosen, J. M. (1995) *Proc. Natl. Acad. Sci. USA* **92**, 3439–3443.
20. Bostwick, D. G. (2000) *Curr. Urol. Rep.* **1**, 65–70.
21. Magi-Galluzzi, C., Montironi, R., Cangi, M. G., Wishnow, K. & Loda, M. (1998) *Virchows Arch.* **432**, 407–413.
22. Signoretti, S., Waltregny, D., Dilks, J., Isaac, B., Lin, D., Garraway, L., Yang, A., Montironi, R., McKeon, F. & Loda, M. (2000) *Am. J. Pathol.* **157**, 1769–1775.
23. Goberdhan, D. C., Paricio, N., Goodman, E. C., Mlodzik, M. & Wilson, C. (1999) *Genes Dev.* **13**, 3244–3258.
24. Huang, H., Potter, C. J., Tao, W., Li, D. M., Brogiolo, W., Hafen, E., Sun, H. & Xu, T. (1999) *Development* **126**, 5365–5372.
25. Malstrom, S., Tili, E., Kappes, D., Ceci, J. D. & Tschlis, P. N. (2001) *Proc. Natl. Acad. Sci. USA* **98**, 14967–14972.
26. Condorelli, G., Drusco, A., Stassi, G., Bellacosa, A., Roncarati, R., Iaccarino, G., Russo, M. A., Gu, Y., Dalton, N., Chung, C., et al. (2002) *Proc. Natl. Acad. Sci. USA* **99**, 12333–12338.
27. Shioi, T., McMullen, J. R., Kang, P. M., Douglas, P. S., Obata, T., Franke, T. F., Cantley, L. C. & Izumo, S. (2002) *Mol. Cell. Biol.* **22**, 2799–2809.
28. Bernal-Mizrachi, E., Wen, W., Stahlhut, S., Welling, C. M. & Permutt, M. A. (2001) *J. Clin. Invest.* **108**, 1631–1638.
29. Stambolic, V., Tsao, M. S., Macpherson, D., Suzuki, A., Chapman, W. B. & Mak, T. W. (2000) *Cancer Res.* **60**, 3605–3611.
30. Gu, Z., Thomas, G., Yamashiro, J., Shintaku, I. P., Dorey, F., Raitano, A., Witte, O. N., Said, J. W., Loda, M. & Reiter, R. E. (2000) *Oncogene* **19**, 1288–1296.
31. Dubey, P., Wu, H., Reiter, R. E. & Witte, O. N. (2001) *Cancer Res.* **61**, 3256–3261.
32. Levedakou, E. N., Strohmeyer, T. G., Effert, P. J. & Liu, E. T. (1992) *Int. J. Cancer* **52**, 534–537.
33. Coleman, R. E., Mashiter, G., Fogelman, I., Whitaker, K. D., Caleffi, M., Moss, D. W. & Rubens, R. D. (1988) *Eur. J. Cancer Clin. Oncol.* **24**, 1211–1217.
34. Zundel, W., Schindler, C., Haas-Kogan, D., Koong, A., Kaper, F., Chen, E., Gottschalk, A. R., Ryan, H. E., Johnson, R. S., Jefferson, A. B., et al. (2000) *Genes Dev.* **14**, 391–396.
35. Treins, C., Giorgetti-Peraldi, S., Murdaca, J., Semenza, G. L. & Van Obberghen, E. (2002) *J. Biol. Chem.* **277**, 27975–27981.
36. Moriyama, N., Kurimoto, S., Miyata, N., Yamaura, H., Yamazaki, R., Sudoh, K., Inagaki, O., Takenaka, T. & Kawabe, K. (1996) *Gen. Pharmacol.* **27**, 1061–1065.
37. Nelson, J. B., Chan-Tack, K., Hedican, S. P., Magnuson, S. R., Oppenorth, T. J., Bova, G. S. & Simons, J. W. (1996) *Cancer Res.* **56**, 663–668.